Title

Efficient derivation of cortical glutamatergic neurons from human pluripotent stem cells: A model system to study neurotoxicity in Alzheimer's disease

Permalink

https://escholarship.org/uc/item/57d948k1

Authors

Vazin, Tandis
Ball, K Aurelia
Lu, Hui
et al.

Publication Date

2014-02-01

DOI

10.1016/j.nbd.2013.09.005

Peer reviewed

Efficient derivation of cortical glutamatergic neurons from human pluripotent stem cells: A model system to study neurotoxicity in Alzheimer's disease

Tandis Vazin[a,b,f], K. Aurelia Ball[c,f], Hui Lu[b,d,f], Teresa Head-Gordon[a,c,e,f], Mu-ming Poo[b,d,f] and David V. Schaffer[a,b,f]

[a] The Department of Chemical and Biomolecular Engineering, the Department of Bioengineering

[b] Helen Wills Neuroscience Institute

[c] Graduate Group in Biophysics

[d] Division of Neurobiology, Department of Molecular and Cell Biology

[e] Department of Chemistry

[f] University of California, Berkeley, California 94720, USA.

Corresponding author: David V. Schaffer, 278 Stanley Hall, University of California, Berkeley, California 94720, USA. E-mail: schaffer@berkeley.edu

Number of pages: 32   Number of figures: 8   Number of tables: 1

Abstract: 249   Introduction: 500   Discussion : 1283

Conflict of Interest: The authors declare no competing financial interests.

Abstract

Alzheimer's disease (AD) is among the most prevalent forms of dementia affecting the aging population, and pharmacological therapies to date have not been successful in preventing disease progression. Future therapeutic efforts may benefit from the development of models that enable basic investigation of early disease pathology. In particular, disease-relevant models based on human pluripotent stem cells (hPSCs) may be promising approaches to assess the impact of neurotoxic agents in AD on specific neuronal populations and thereby facilitate the development of novel interventions to avert early disease mechanisms. We implemented an efficient paradigm to convert hPSCs into enriched populations of cortical glutamatergic neurons emerging from dorsal -forebrain neural progenitors, aided by modulating Sonic hedgehog (Shh) signaling. Since AD is generally known to be toxic to glutamatergic circuits, we exposed glutamatergic neurons derived from hESCs to an oligomeric pre-fibrillar forms of Aβ known as "globulomers", which have shown strong correlation with the level of cognitive deficits in AD. Administration of such Aβ oligomers yielded signs of the disease, including cell age-dependent binding of Aβ and cell death in the glutamatergic populations. Furthermore, Aβ-induced toxicity was selective for glutamatergic rather than GABAeric neurons present in our cultures, consistent with previous findings in postmortem human AD brain. This *in vitro* model of cortical glutamatergic neurons thus offers a system for future mechanistic investigation and therapeutic development for AD pathology using human cell types specifically affected by this disease.

Introduction

AD is a neurodegenerative disorder characterized by an abundance of Aβ peptides generated from ~~amyloid precursor~~ abnormal cleavage of the transmembrane amyloid precursor protein by membrane-associated secretases (Murphy and LeVine, 2010). The development of AD pathology precedes cognitive symptoms and diagnosis by many years (Lazarczyk et al., 2012), presenting challenges for studying early disease stages to aid in the discovery of preventive drugs.

Over the past decade numerous transgenic animal models of AD have been generated to aid in understanding mechanisms of the disease in humans (Gotz and Ittner, 2008). However, such animals must express multiple pathological proteins at levels higher than endogenous genes to exhibit AD pathology, which highlight the value of developing models that could enable investigation in human cells with gene expression patterns closer to endogenous levels. For example, *in vitro* models derived from hPSCs offer strong platforms for basic research and subsequent therapeutic development for early stages of AD. However, tapping into this potentially exciting new class of disease models requires efficient differentiation of hPSCs into neurons affected by AD. In particular, glutamatergic neurons are severely afflicted in the cerebral cortex, ~~By comparison, earlier~~whereas studies of human postmortem AD brain suggest that GABAergic neurons are spared from death (Rossor et al., 1982). ~~and D~~disruption of glutamatergic neuronal~~their~~ circuits is associated with the hallmark memory deficits of AD (Francis et al., 1993; Greenamyre et al., 1988). ~~.~~ By comparison, earlier studies of human postmortem AD brain suggest that GABAergic neurons are spared from death (Rossor et al., 1982)and possibly the resulting disregulation due to exhibitory/inhibitory imbalance (Rissman, Robert A., and William C. Mobley. "Implications for treatment: GABAA receptors in aging, Down syndrome and Alzheimer's disease." Journal of neurochemistry 117.4 (2011): 613-622), is

associated with the hallmark memory deficits of AD (Francis et al., 1993; Greenamyre et al., 1988). Hence, renewable sources of glutamatergic neurons derived from hPSCs would hold considerable promise as human disease models of AD. To date, the sensitivity of human cortical glutamatergic neurons to Aβ has not been studied within *in vitro* models. Given the differences in disease symptoms between familial AD and corresponding animal models (Gotz and Ittner, 2008), we have thus developed an hPSC-based system to examine how Aβ neurotoxicity affects enriched populations of human cortical glutamatergic neurons and provide a relative comparison to the GABAergic population in our cultures.

During development, glutamatergic neurons are generated from the dorsal telencephalon, whereas GABAergic neurons emerge from the ventral telencephalic region (Wilson and Rubenstein, 2000), due in part to Shh-mediated patterning. Here, we show that hESCs and iPSCs differentiated to a dorsal phenotype, with the aid of Shh pathway inhibition and stimulation with FGF-2, primarily give rise to glutamatergic neurons. In contrast, without Shh inhibition, neuronal progenitor cells (NPCs) adapted a ventral phenotype and mainly gave rise to a GABAergic fate.

AD is primarily characterized by Aβ plaques; however, amyloid plaque load show a weak correlation with dementia in AD (Naslund et al., 2000). By comparison, soluble Aβ oligomer levels correlate more closely with AD pathology (Kuo et al., 1996). and more recently a pre-fibrillar oligomeric form ~~Thus, a stable oligomeric Aβ called "Aβ globulomers" has been prepared and increasingly studied (Barghorn et al., 2005, Gellermann et al., 2008).~~ known as the "globulomer" (Barghorn et al., 2005, Gellermann et al., 2008) were found to inhibit calcium uptake by neuronal cells and to contribute to memory loss in lab animals. While human AD brain neuropathology studies show elevated levels of Aβ oligomers surrounding cortical neuronal processes, which may cause synaptic impairment (Viola et al., 2008), the differential neurotoxic

effects of these oligomers on different human cortical neuronal populations remain to be elucidated. Such results may enhance our understanding of the contribution of this toxic species to the disease process and aid future elucidation of molecular mechanisms for its actions.

In this study, the derivation of human cortical cultures primarily comprised of glutamatergic neurons enabled investigation of the recently proposed role of Aβ "globulomers" in AD pathology. Specifically, this intermediate form of Aβ was toxic to human glutamatergic neurons in a cell culture age-dependent manner. Furthermore, the results interestingly show that Aβ globulomers exert a distinctive neurotoxicity in glutamatergic neurons in comparison to the GABAergic neuronal populations.

Materials and Methods

Cell culture

The H1 (WiCell) and HSF6 (UC San Francisco) hESC lines, and the MSC and fibroblast derived iPSC lines (a kind gift from George Q. Daley, Children's Hospital Boston, Boston, MA), were cultured on Matrigel-coated cell culture plates (BD) in mTeSR1 maintenance medium (Stem Cell Technologies). NPCs were isolated from the hippocampus of adult female Fischer 344 rats (Palmer et al., 1999) and cultured in medium containing DMEM/F12 (Invitrogen) supplemented with N2 (Invitrogen) and 20 ng/ml FGF-2 (Peprotech). Neuronal differentiation of adult rat NPCs was achieved by withdrawing FGF-2 and adding 1 µM retinoic acid and 5 µM forskolin for 5 days.

Cortical differentiation of human pluripotent stem cells

In adherent conditions, hPSCs were seeded at a density of 5×10^4 cells/cm^2 in growth medium. At 50% confluence, the medium was gradually changed to neural basal medium (Invitrogen)

containing N2 and B27 (Invitrogen). SMAD signaling inhibitors LDN193189 (Stemgent, 1 µM) and SB432542 (Tocris Biosciences, 10 µM) were added from day 1 to day 7 of neural induction. Cyclopamine (Calbiochem, 400 ng/ml) and FGF-2 (Peprotech, 10 ng/ml) were added from days 3-14 of differentiation. After 12-14 days, cells were mechanically passaged into poly-L-ornithine (Sigma Aldrich) and laminin (Invitrogen, 20µg/ml) coated plates and allowed to undergo maturation for 3-6 weeks. BDNF (10 ng/ml, Peprotech) was added to cultures one week after initiation of neuronal maturation. For EB mediated neural differentiation, PSCs were aggregated for 4 days in ultra low-attachment plates (Corning) and then seeded on Matrigel-coated plates. Cyclopamine (5 µM) and FGF-2 (10 ng/ml) were added to the cultures the following day until day 12 of neural induction. At day 14, structures with a rosette-like morphology were mechanically isolated and plated on poly-L-ornithine and laminin coated plates and allowed to undergo neuronal maturation for 4 weeks. BDNF (10 ng/ml) was added to the cultures one week after rosette isolation.

Gene expression analysis by RT-PCR

Complementary DNA was synthesized from 1 µg total RNA, isolated at day 12 of neural induction and day 40 of neuronal maturation, using random primers and MultiScribe Reverse Transcriptase (Applied Biosystems) in a 20 µl reaction according to the manufacturer's recommendations. The PCR analysis was carried out with Taq DNA polymerase (New England Biolabs). Equal amounts of RNA were tested in PCR reactions under the same conditions to verify the absence of amplification of genomic DNA. The housekeeping gene glyceraldehyde-3-phosphate dehydrogenase (G3PDH) was amplified as an internal control in gene expression analysis. Primer sequences (Table 1) were obtained from the PrimerBank website (http://pga.mgh.harvard.edu/primerbank/) and synthesized by Life Technologies.

Immunocytochemistry

Cultures were fixed with 4% paraformaldehyde or 3% paraformaldehyde and 2% glutaraldehyde for 10-15 min. The primary antibodies used were: mouse anti-nestin (1:50; R & D Research), rabbit anti-Pax6 (1:200; Covance), rabbit anti-BF1 (1:100, Abcam), mouse anti-Otx2 (1:50, R&D Systems), mouse anti-MAP2 (1:500, BD Biosciences), rabbit anti-glutamate (1:1500, Sigma Aldrich,), rabbit anti-GBA (1:2000, Sigma Aldrich), rabbit anti VGluT1 (1:3000, Synaptic Systems), rabbit anti-TBR1 (1:1000, Millipore), rabbit anti-CUX1 (1:1000, Santa Cruz Biotechnology), rat anti-CTIP2 (1:1000, Abcam), rabbit anti-cleaved caspase 3 with Alexa Fluor 488 Conjugate (1:100, Cell Signaling). Cultures were (with the exception of caspase 3) incubated with fluorescent-labeled secondary Alexa 594-conjugated anti-rabbit and Alexa 488-conjugated anti-mouse antibodies in PBS containing 1% BSA for 1 hr (1:1000, Invitrogen). Cultures were counter-stained with DAPI (Molecular probes) and imaged using a Zeiss Axio Observer A1 inverted microscope.

Electrophysiology

Whole-cell recording was made from neurons after 50 days of neuronal maturation using a patch clamp amplifier (MultiClamp 700B, Axon Instr.) under infrared differential interference contrast optics. Microelectrodes were made from borosilicate glass capillaries, with a resistance of 4-5 $M\Omega$. To apply glutamate, air pulses (10 ms duration at 1 Hz) were applied by Picrospritzer III (Parker Hannifin) to a glass pipette with the tip of ~ 5 µm in diameter. Generally, EPSPs induced by puffed glutamate were recorded at -70 mV in current-clamp mode. For recording action potentials, cells were held at -70 mV in voltage-clamp mode. The intracellular solution for whole-cell recording contained 140 mM potassium gluconate, 5 mM KCl, 10 mM HEPES, 0.2 mM EGTA, 2 mM $MgCl_2$, 4 mM MgATP, 0.3 mM Na_2GTP and 10 mM Na_2-phosphocreatine, pH

7.2 (with KOH). Series resistance (15-30 MΩ) and input resistance (~ 200 MΩ) were monitored throughout the whole-cell recording. All experiments were done at the room temperature (22 $^{\circ}$C–24 $^{\circ}$C).

Globulomer Preparation

The Aβ42 globulomer was prepared as described (Barghorn et al., 2005; Yu et al., 2009). Alkaline pretreatment of Aβ42 and preparation of low molecular weight Aβ by filtration protocols were used before beginning the globulomer preparation as previously described (Yu et al., 2009). After the 18-20 h incubation, the globulomer sample were concentrated to ~500 μM via centrifugation and dialyzed into PBS before centrifuging the sample at 10,000 g for 10 min to remove aggregates in the pellet. The supernatant was saved, and the absorbance was measured at 276 nm wavelength to measure the concentration (extinction coefficient = 1390 M^{-1} cm^{-1}).

Aβ42 Monomer Preparation

The alkaline pretreatment of Aβ42 and preparation of LMW Aβ by filtration protocols outlined by Teplow (Teplow, 2006) were also used to prepare a monomeric solution of the peptide. This involved dissolving 1 mg of the lyophilized peptide in 2 mL of 2 mM sodium hydroxide, sonicating for 2 minutes, and lyophilizing. This lyophilized peptide was then dissolved in 0.166 ml hexafluoroisopropanol (HFIP) to break any existing hydrogen bonds and prevent aggregation.

Statistics

Differences in percentages of cells obtained from three independent experiments were tested by analysis of variance followed by pair-wise comparisons of group means using the Tukey-Kramer

method for multiple comparisons. Levels of significance are indicated by asterisks on the line graphs and figure legends. Differences were considered significant at $P < 0.05$.

Results

Derivation of telencephalic neural progenitor cells

As illustrated in Figure 1A, we first used BMP/SMAD signaling inhibitors to efficiently induce hPSC differentiation into a neural lineage (Chambers et al., 2009), and consistent with its role in (Wilson and Rubenstein, 2000) development, inhibition of the Shh signaling pathway by cyclopamine directed the resulting NPCs to a dorsal phenotype. In addition to its ventralizing effect, Shh can exert a proliferative effect on NPCs (Lai et al., 2003), and accordingly we observed a decrease in the proliferation and survival of NPCs in the presence of cyclopamine. To mitigate this loss of viability, the mitogen FGF-2, also known to exert an instructive role during telencephalic development (Ideguchi et al., 2010; Paek et al., 2009; Robel et al., 1995), was added and found to reverse the impact of cyclopamine on cell survival and proliferation (data not shown). This approach (Figure 1A) first converted hESC cultures to a neural lineage at a high rate, as determined by nestin and Pax6 expression (Figure 1B, C). Subsequent inhibition of Shh activity and addition of FGF-2 led to a significant increase in expression of the forebrain regionalization marker OTX2 and the telencephalic-restricted transcription factor BF1/FoxG1 (Figure 1B, C), as compared to cultures with intact Shh signaling. To further examine the regional identity of the resulting NPCs, expression of markers associated with the ventral and dorsal forebrain was investigated. Shh signal inhibition during neural induction resulted in upregulation of the dorsal marker Emx1 and downregulation of DLX2, a marker exclusively expressed in the developing ventral telencephalon.

Subsequent neuronal lineage analysis of the dorsally patterned telencephalic NPCs revealed that approximately 74% of neurons acquired a glutamatergic phenotype, whereas GABAergic neurons comprised only 20% of the neuronal population (Figure 2A, C). Conversely, ventral

NPCs developed in the absence of cyclopamine gave rise to approximately 18% and 62% glutamatergic and GABAergic neurons, respectively (Figure 2B, C). To further confirm the glutamatergic phenotype, we investigated the expression of the T-domain transcription factor (TBR1), which is restricted to glutamatergic neurons and excluded from GABAergic neurons in the neocortex (Hevner et al., 2001). The results illustrated clear TBR1 expression in the majority of neurons developed from dorsal NPCs (Figure 2D). Expression of VGluT1, which enables quantal release of glutamate, was also detected (Figure 2E). In the dorsally patterned, mature cortical cultures, neurons were often positive for CUX1, a marker of cortical projection neurons in upper layers (2-4) (Figure 2F), as well as CTIP2, a transcription factor enriched in deep layers (5-6) (Figure 2G). The differential expression of VGluT1 and TBR1 resulting from differentiation with or without Shh inhibition was further indicated by reverse transcription polymerase chain reaction (RT-PCR) analysis (Figure 2H). To test the robustness of the differentiation strategy, we also used a protocol that involved embryoid body formation – rather than SMAD inhibition in adherent cultures – and with Shh signaling inhibition again successfully generated dorsally patterned neuronal populations expressing glutamate and VGluT1 (Figure 3A-C). However, while the fraction of hESC-derived neurons restricted to a glutamatergic fate was comparable to the adherent conditions, the latter culture led to a higher overall proportion of neurons within the culture. Subsequent studies were therefore conducted using the monolayer approach.

The pioneering work by Yamanaka and colleagues (Takahashi et al., 2007) enabling conversion of somatic cells to induced pluripotent stem cells (iPSCs) has in the recent years offered the unique potential to model human diseases with patient-derived cells (Park et al., 2008) . To explore the general potential of iPSCs for differentiating into cortical neurons, we analyzed whether the differentiation paradigm established for hESCs could extend to iPSCs. Similar to

hESCs, in the presence of cyclopamine mesenchymal stem cell (MSC) derived iPSCs (Park et al., 2008) adopted a dorsal phenotype, and glutamatergic differentiation occurred at the expense of GABAergic development (Figure 4A-C). Additionally, TBR1 and VGluT1 expression further indicated cortical glutamatergic differentiation (Figure 4D-F).

Electrophysiological assessment of cortical neurons

To examine the functional activity of the differentiated neurons, electrophysiological recordings were performed using whole-cell patch clamping after 52 days of differentiation. Upon current injection, the dorsally patterned neurons generated from hESCs showed the capacity to fire numerous action potentials (Figure 5A). In addition, depolarizing voltage pulses evoked inward sodium currents, contributing to membrane excitability followed by an outward current (Figure 5B). Moreover, the voltage-gated sodium channel blocker tetrodotoxin (TTX) blocked inward currents, providing further evidence for the presence of functional sodium channels that are responsible for action potential generation and propagation of excitatory signals by evoking release of glutamate in presynaptic glutamatergic terminals (Figure 5B). Consistent with immunocytochemical analysis of glutamatergic marker expression (Fig 2A, D), glutamate application elicited a rapidly activating inward current and further confirmed the glutamatergic neuronal phenotype (Figure 5C). The iPSC-derived, dorsally regionalized forebrain neurons also developed into electrophysiologically mature neurons as measured by the ability to generate action potentials (Figure 5D) and voltage-sensitive inward and outward currents (Figure 5E).

Evaluation of human cortical glutamatergic neurons as a model for AD investigation

We generated a soluble and highly stable form of Aβ oligomers termed globulomers, which are excluded from polymerization and assembly into larger fibrils (Barghorn et al., 2005). Initially, neurons derived from adult rat hippocampal progenitors were used to determine a concentration

range of this species that may be toxic, and globulomer preparations from Aβ peptide concentrations ranging from 1-5 µM were sufficient to induce cell death within 48 hours (Figure 6A).

When hESC-derived cortical cultures primarily comprised of glutamatergic neurons were treated with 2 µM globulomers, clear neuronal cell death initiated after 72 hours (Figure 6B). Analysis using caspase-3 as an apoptotic marker showed a progressive increase in glutamatergic neuron death with increasing Aβ globulomer concentration (Figure 6C, D), and the fraction of neurons (MAP2+) that were glutamatergic also progressively decreased (Figure 6E). Finally, the overall fraction of cells in the culture that were MAP2+ and that were glutamate+/MAP2+ decreased in parallel, suggesting a selective neurotoxicity of Aβ globulomers against these human cortical glutamatergic neurons (Figure 6F). By comparison, cultures treated with the same concentrations of the monomeric, non-toxic form of Aβ peptide did not show activation of caspase-3.

We also immunostained for the presence of this pre-fibrillar form of Aβ to further investigate cellular interactions, using an antibody against the Aβ fibrillar oligomeric form that also binds the soluble Aβ globulomers due to some structural similarity (Glabe, 2008). In agreement with previous studies (Barghorn et al., 2005; Verdier et al., 2004), globulomer aggregates were tightly associated with the neuronal cell membrane (Figure 7A). Similarly, iPSC-derived neurons exhibited Aβ globulomer binding and subsequent apoptosis (data not shown). We also investigated whether neurons that had matured longer in culture may respond differentially to the Aβ globulomers, since organismal aging is the most prominent risk factor for AD, and neuronal lifetime in culture may embody some aspects of aging (Lesuisse and Martin, 2002). When hESC-derived cortical neuronal populations were matured for an additional 33 days, for a total of 72 days after the initiation of differentiation, Aβ binding to the plasma membrane and the dendritic

spines was significantly increased (Figure 7B). Specifically, quantitative assessments of 100 neurons showed an increase in the average number of bound globulomer aggregates per neuron from 3 ± 1 in younger cultures to 8 ± 2 in old (P < 0.001), indicating that increased cell culture maturation time could offer a platform to examine how changes in neuronal membrane properties with time lead to increases in Aβ binding and pathology. Collectively, these findings illustrate that cortical neuronal cultures can be used *in vitro* to emulate and investigate AD phenotypes.

Examination of Aβ-induced neurotoxicity in glutamatergic and GABAergic populations

The extent to which specific sets of neurons in the cerebral cortex are susceptible to Aβ ~~oligomer~~ globulomer binding and toxicity is unknown. To study neuronal phenotype sensitivities to Aβ, we exposed mature hESC-derived cultures primarily comprised of glutamatergic or GABAergic neurons to Aβ globulomer and assessed globulomer binding and neuronal cell death after 72 hr. The levels of globulomer bound to MAP2-expressing neurons was significantly higher in glutamatergic neuronal cultures, differentiated from dorsal NPCs, than primarily GABAergic neurons, derived from ventral NPCs (Figures 8A-B, E). Likewise, gluatamatergic and GABAergic cultures exhibited substantially different levels of apoptotic cell death (Figure 8C-E). In glutamatergic cultures exposed to Aβ, caspase-3 activation occurred in 61% of cells, compared to 33% in untreated conditions, and the fraction of overall MAP2+ neurons decreased from 56 to 31% (representing an overall 55% decrease) in response to Aβ treatment. In contrast, the GABAergic population was more resistant to Aβ, as the fraction of neurons decreased by only 17% after treatment, and neuronal caspase 3 staining was the same in treated vs. untreated cultures (Figure 8E).

Discussion

Numerous transgenic animal models of AD have been generated to aid in understanding mechanisms of this human disease (Gotz and Ittner, 2008), and while these models continue to provide valuable insights into disease mechanisms, non-human systems often do not fully emulate human pathophysiology as evidenced by the poor correlation between preclinical models and human clinical trials (LaFerla and Green, 2012). Analogously, overexpressing genes that influence amyloidogenesis in neurons derived from immortalized cell lines, such as the frequently used human neuroblastoma line SH-SY5Y (Belyaev et al., 2010), may not represent an accurate model to study AD as these cells are quite different from neurons that degenerate in human AD brain. Finally, tissue from AD patients is both heterogeneous and limited. Such challenges can potentially be addressed by using models of hPSC-derived neuronal phenotypes that undergo degeneration in AD for basic investigation or therapeutic development. In this study, we established an efficient differentiation paradigm to generate human glutamatergic neurons and begun to evaluate their potential as an AD model.

Recent studies (Israel et al., 2012; Qiang et al., 2011; Yagi et al., 2012) have successfully generated neurons from fibroblasts of familial and sporadic AD patients by cellular reprogramming. That said, neuronal models based on iPSCs or direct reprogramming of cells from AD patients likely preclude the possibility of introducing a pathological AD environment to already mature and healthy neuronal populations, and thereby complicate efforts to develop preventive measures at early stages of the disease. The cholinergic system is also affected by AD (Francis et al., 1999), and a model of cholinergic neurons derived from hESCs has recently been established (Bissonnette et al., 2011). However, human cortical glutamatergic neurons, which are strongly involved in the neuropathology of AD (Francis et al., 1993; Greenamyre et al., 1988), have remained largely unexplored in biomedical investigations of this disease.

During forebrain development, Shh signaling contributes to the establishment of dorsal and ventral cortical regions, leading to the generation of glutamatergic and GABAergic neurons, respectively (Ericson et al., 1995; Wilson and Rubenstein, 2000). Based on these findings, differentiation protocols of ESCs have used Shh pathway inhibition to obtain NPCs with distinct telencephalic regional identities (Gaspard et al., 2008; Shi et al., 2012). However, a recent contrasting study indicated that human ESCs undergo a self-organized formation of dorsal telencephalic neural progenitors without extrinsic inhibition of the Shh pathway (Li et al., 2009).

In this study, we show that active manipulation with a Shh antagonist can lead to a more efficient specialization of dorsal telencephalic NPCs, and in turn efficiently yield glutamate expressing neurons. Conversely, in the absence of Shh inhibition, the resulting NPCs adapted a ventral phenotype and primarily gave rise to GABAergic neurons. In addition, FGF-2 exerts a wide range of activities during early brain development including stimulation of neural precursor proliferation, neuronal differentiation, neurite outgrowth of hippocampal and cortical neurons, and enhancement of neuronal survival (Gremo and Presta, 2000). FGF-2 may also play a role in forebrain patterning, as it has been suggested to regulate Otx2 expression in the developing telencephalon (Robel et al., 1995). In contrast to the previous studies of ESC cortical differentiation (Gaspard et al., 2008; Shi et al., 2012), we found that FGF-2 could be used to greatly enhance forebrain NPC survival and proliferation, as well as promote a downstream increase in the number of human cortical neurons.

We used the resulting cortical glutamatergic neurons, derived from the H1 hESC line as well as a MSC-iPSC line, to study AD pathology *in vitro* by showing severe toxicity for a pre-fibrillar form of Aβ that may be present in patients suffering from AD (Kuo et al., 1996). Interestingly, the glutamatergic model illustrated enhanced binding of Aβ globulomers to individual neurons

with increased time in culture, which may have some parallels with neuronal aging *in vivo* (Lesuisse and Martin, 2002). The mechanisms and binding partners involved in the association of Aβ oligomers with cortical neurons have not been identified, though a number of membrane associated proteins – including NMDA receptors, integrins, and proteoglycans – have been identified as potential binding proteins in various types of neurons (Verdier et al., 2004). An alternative hypothesis for Aβ-induced cytotoxicity involves age-related disruption of the cell surface membrane through alterations of the membrane lipid layer fluidity that eventually lead to apoptotic or necrotic cell death (Igbavboa et al., 1996; Kremer et al., 2000). In either case, the model presented in this study may offer a platform for advancing our understanding of age-related association and binding of Aβ to the plasma membranes as a potential point of intervention. Future studies may also help delineate how *in vitro* cellular aging may correlate with *in vivo* human age, such that stem cell derived neuronal models could lend insights into age-related pathology in humans.

Our Aβ neurotoxicity analysis indicated a selective pathology against glutamatergic neurons, as the fraction of neurons of this phenotype decreased with increasing Aβ concentrations. This effect may be related to their capacity to bind the globulomers (Figure 8E). In fact, it has been suggested by studies performed in neuronal cell lines and rat primary hippocampal and cortical cultures that differential sensitivity to Aβ is associated with cell membrane Aβ binding (Simakova and Arispe, 2007). However, the binding affinity and selective sensitivity of different type of neurons to neurotoxic effects of Aβ remains a matter of debate and must be studied in greater detail.

 Hippocampal GABAergic neurons are susceptible to Aβ toxicity *in vitro* and decrease in number in the AD TgCRND8 mouse (Krantic et al., 2012; Pike and Cotman, 1993), and small

GABAergic neurons were vulnerable to Aβ pentapeptide in primary rat basal forebrain cultures (Pakaski et al., 1998). Other studies in mice overexpressing Apolipoprotein E4, a major genetic risk factor for AD, have shown a tauopathy mediated impairment of hippocampal GABAergic interneurons (Andrews-Zwilling et al., 2010), which may be Aβ-independent (Huang, 2010). By contrast, cortical GABAergic neurons were relatively spared in a study of postmortem tissue from AD patients (Rossor et al., 1982). A recent study suggested that aberrant network activity in human APP transgenic mice may arise from decreased expression of a voltage-gated sodium channel subunit in cortical parvalbumin subtype GABAergic interneurons (Verret et al., 2012), though GABAergic neurodegeneration was not specifically examined in this study. Given stark differences in the sensitivity of human and mouse brain to pathological alleles from familial forms of AD, it is important to examine Aβ biology and pathology in the types of human neurons directly impacted by AD. To our knowledge, however, the cell-type specific behavior of human cortical neurons has not been explored in an AD neurotoxic environment.

To shed some light on neuronal phenotype-specific vulnerability in AD, we present a human cell model of glutamatergic and GABAergic neuronal cultures and illustrate that the glutamatergic neurons are comparatively more susceptible to Aβ toxicity. These results with human cells agree more closely with the cerebral cortex of postmortem human AD patients (Rossor et al., 1982) than with animal studies conducted to date.

The cortical culture systems presented in this study provides an opportunity to study the underlying mechanisms of the differential response of human neuronal phenotypes to the most neurotoxic agent in AD. Future advances in the generation and assessment of neurons representative of the distinct layers of the cortex may further aid studies of neuronal vulnerability

to AD pathology, and in general hPSC-derived cortical neuronal cultures may lay the groundwork for more effective discovery of AD diagnostics or pharmacological intervention.

Conclusions

We have examined the effects of a pre-fibrillar form of Aβ on human pluripotent stem cell derived glutamatergic neurons, which comprise a large fraction of the human cortical regions that undergo severe degeneration in AD. Our study clearly shows a human cortical neuronal phenotype–dependent binding of and susceptibility to Aβ globulomers. The ability to reproducibly generate large quantities of different human neuronal subtypes will help investigations of cellular and biochemical dynamics during early to late stages of AD-induced neurodegeneration, which may aid in the identification of new diagnostic markers and ultimately new preventive treatments.

References

Andrews-Zwilling, Y., et al., 2010. Apolipoprotein E4 causes age- and Tau-dependent impairment of GABAergic interneurons, leading to learning and memory deficits in mice. J Neurosci. 30, 13707-17.

Barghorn, S., et al., 2005. Globular amyloid beta-peptide oligomer - a homogenous and stable neuropathological protein in Alzheimer's disease. J Neurochem. 95, 834-47.

Belyaev, N. D., et al., 2010. The Transcriptionally Active Amyloid Precursor Protein (APP) Intracellular Domain Is Preferentially Produced from the 695 Isoform of APP in a beta-Secretase-dependent Pathway. Journal of Biological Chemistry. 285, 41443-41454.

Bissonnette, C. J., et al., 2011. The controlled generation of functional basal forebrain cholinergic neurons from human embryonic stem cells. Stem Cells. 29, 802-11.

Chambers, S. M., et al., 2009. Highly efficient neural conversion of human ES and iPS cells by dual inhibition of SMAD signaling. Nat Biotechnol. 27, 275-80.

Ericson, J., et al., 1995. Sonic hedgehog induces the differentiation of ventral forebrain neurons: a common signal for ventral patterning within the neural tube. Cell. 81, 747-56.

Francis, P. T., et al., 1999. The cholinergic hypothesis of Alzheimer's disease: a review of progress. J Neurol Neurosurg Psychiatry. 66, 137-47.

Francis, P. T., et al., 1993. Cortical pyramidal neurone loss may cause glutamatergic hypoactivity and cognitive impairment in Alzheimer's disease: investigative and therapeutic perspectives. J Neurochem. 60, 1589-604.

Gaspard, N., et al., 2008. An intrinsic mechanism of corticogenesis from embryonic stem cells. Nature. 455, 351-7.

Glabe, C. G., 2008. Structural classification of toxic amyloid oligomers. J Biol Chem. 283, 29639-43.

Gotz, J., Ittner, L. M., 2008. Animal models of Alzheimer's disease and frontotemporal dementia. Nat Rev Neurosci. 9, 532-44.

Greenamyre, J. T., et al., 1988. Glutamate transmission and toxicity in Alzheimer's disease. Prog Neuropsychopharmacol Biol Psychiatry. 12, 421-30.

Gremo, F., Presta, M., 2000. Role of fibroblast growth factor-2 in human brain: a focus on development. Int J Dev Neurosci. 18, 271-9.

Hevner, R. F., et al., 2001. Tbr1 regulates differentiation of the preplate and layer 6. Neuron. 29, 353-66.

Huang, Y., 2010. Abeta-independent roles of apolipoprotein E4 in the pathogenesis of Alzheimer's disease. Trends Mol Med. 16, 287-94.

Ideguchi, M., et al., 2010. Murine embryonic stem cell-derived pyramidal neurons integrate into the cerebral cortex and appropriately project axons to subcortical targets. J Neurosci. 30, 894-904.

Igbavboa, U., et al., 1996. Increasing age alters transbilayer fluidity and cholesterol asymmetry in synaptic plasma membranes of mice. J Neurochem. 66, 1717-25.

Israel, M. A., et al., 2012. Probing sporadic and familial Alzheimer's disease using induced pluripotent stem cells. Nature. 482, 216-20.

Krantic, S., et al., 2012. Hippocampal GABAergic neurons are susceptible to amyloid-beta toxicity in vitro and are decreased in number in the Alzheimer's disease TgCRND8 mouse model. J Alzheimers Dis. 29, 293-308.

Kremer, J. J., et al., 2000. Correlation of beta-amyloid aggregate size and hydrophobicity with decreased bilayer fluidity of model membranes. Biochemistry. 39, 10309-18.

Kuo, Y. M., et al., 1996. Water-soluble Abeta (N-40, N-42) oligomers in normal and Alzheimer disease brains. J Biol Chem. 271, 4077-81.

LaFerla, F. M., Green, K. N., 2012. Animal models of Alzheimer disease. Cold Spring Harb Perspect Med. 2.

Lai, K., et al., 2003. Sonic hedgehog regulates adult neural progenitor proliferation in vitro and in vivo. Nat Neurosci. 6, 21-7.

Lazarczyk, M. J., et al., 2012. Preclinical Alzheimer disease: identification of cases at risk among cognitively intact older individuals. BMC Med. 10, 127.

Lesuisse, C., Martin, L. J., 2002. Long-term culture of mouse cortical neurons as a model for neuronal development, aging, and death. J Neurobiol. 51, 9-23.

Li, X. J., et al., 2009. Coordination of sonic hedgehog and Wnt signaling determines ventral and dorsal telencephalic neuron types from human embryonic stem cells. Development. 136, 4055-63.

Naslund, J., et al., 2000. Correlation between elevated levels of amyloid beta-peptide in the brain and cognitive decline. Jama-Journal of the American Medical Association. 283, 1571-1577.

Paek, H., et al., 2009. FGF signaling is strictly required to maintain early telencephalic precursor cell survival. Development. 136, 2457-65.

Pakaski, M., et al., 1998. Vulnerability of small GABAergic neurons to human beta-amyloid pentapeptide. Brain Res. 796, 239-46.

Palmer, T. D., et al., 1999. Fibroblast growth factor-2 activates a latent neurogenic program in neural stem cells from diverse regions of the adult CNS. J Neurosci. 19, 8487-97.

Park, I. H., et al., 2008. Disease-specific induced pluripotent stem cells. Cell. 134, 877-86.

Pike, C. J., Cotman, C. W., 1993. Cultured GABA-immunoreactive neurons are resistant to toxicity induced by beta-amyloid. Neuroscience. 56, 269-74.

Qiang, L., et al., 2011. Directed Conversion of Alzheimer's Disease Patient Skin Fibroblasts into Functional Neurons. Cell. 146, 359-371.

Robel, L., et al., 1995. Fibroblast growth factor 2 increases Otx2 expression in precursor cells from mammalian telencephalon. J Neurosci. 15, 7879-91.

Rossor, M. N., et al., 1982. A post-mortem study of the cholinergic and GABA systems in senile dementia. Brain. 105, 313-30.

Shi, Y., et al., 2012. Human cerebral cortex development from pluripotent stem cells to functional excitatory synapses. Nat Neurosci. 15, 477-86, S1.

Simakova, O., Arispe, N. J., 2007. The cell-selective neurotoxicity of the Alzheimer's Abeta peptide is determined by surface phosphatidylserine and cytosolic ATP levels. Membrane binding is required for Abeta toxicity. J Neurosci. 27, 13719-29.

Takahashi, K., et al., 2007. Induction of pluripotent stem cells from adult human fibroblasts by defined factors. Cell. 131, 861-72.

Teplow, D. B., 2006. Preparation of amyloid beta-protein for structural and functional studies. Methods Enzymol. 413, 20-33.

Verdier, Y., et al., 2004. Amyloid beta-peptide interactions with neuronal and glial cell plasma membrane: binding sites and implications for Alzheimer's disease. J Pept Sci. 10, 229-48.

Verret, L., et al., 2012. Inhibitory interneuron deficit links altered network activity and cognitive dysfunction in Alzheimer model. Cell. 149, 708-21.

Viola, K. L., et al., 2008. Why Alzheimer's is a disease of memory: The attack on synapses by A beta oligomers (ADDLs). Journal of Nutrition Health & Aging. 12, 51s-57s.

Wilson, S. W., Rubenstein, J. L., 2000. Induction and dorsoventral patterning of the telencephalon. Neuron. 28, 641-51.

Yagi, T., et al., 2012. Modeling familial Alzheimer's disease with induced pluripotent stem cells. Rinsho Shinkeigaku. 52, 1134-6.

Yu, L., et al., 2009. Structural characterization of a soluble amyloid beta-peptide oligomer. Biochemistry. 48, 1870-7.

Figure Legends

Figure 1. Derivation of ventral and dorsally patterned cortical progenitors. (A) Schematic representation of the paradigm for differentiating hPSCs into cortical NPCs and glutamatergic

neurons. (B) Cultures stained with antibodies against nestin, BF1, and Otx2, under conditions including the Shh signaling inhibitor cyclopamine and FGF-2, cyclopamine alone, or neither factor as indicated in the images. (C) Quantitative analysis of nestin, Pax6, BF1, and Otx2 expression in colonies differentiated in the presence or absence of cyclopamine and FGF-2 showed an increase in forebrain induction in cultures treated with cyclopamine, as indicated by BF1 expression. The differential expression of Otx2 and BF1 in cultures treated with cyclopamine, or with cyclopamine and FGF-2, was significantly different from the control conditions. * = $P<0.01$, **= $P<0.001$. (D) Expression of BF1 and Pax6, as well as upregulation of the dorsal telencephalic marker Emx1 and downregulation of the ventral marker Dlx2, in conditions lacking endogenous Shh signaling was analyzed by RT-PCR. Scale bar: 100 μm.

Figure 2. Glutamatergic and GABAergic differentiation of hESCs. Neuronal lineage analysis of hESC-derived NPCs using antibodies against glutamate and GABA revealed that (A) dorsally regionalized neural progenitors generated by the inhibition of Shh signaling predominantly give rise to glutamatergic neurons at the expense of GABAergic specification, whereas (B) NPCs that developed in the absence of any extrinsic factors mostly adapted a ventral phenotype, giving rise to GABAergic neurons. (C) The average proportion of MAP2+ neuronal cells and the proportions of neurons expressing glutamate or GABA in each condition are presented in bar graphs with error bars indicating standard deviations. The overall difference in the number of glutamatergic and GABAergic neurons in cultures dorsally patterned in the absence of Shh signaling was statistically significant, as compared to conditions where Shh signals remained intact. * = $P < 0.001$. Expression of (D) the transcription factor TBR1 and (E) the vesicular glutamate transporter 1 (VGluT1) was detected in the majority of neurons differentiated from the dorsally patterned neural NPCs. (F) CTIP2 and (G) CUX1 expression confirmed the generation of neurons belonging to the deep and upper cortical layers, respectively. (H) Analysis of

increased expression of TBR1 and VGluT1 in cyclopamine and FGF-2 treated neuronal cultures by RT-PCR. Scale bar: 100 μm.

Figure 3. EB-mediated neuronal differentiation. Cortical differentiation via EB-formation followed by inhibition of the ventralizing effect of Shh resulted in (A) glutamate expression in the majority of MAP+ neurons with (B) a pyramidal morphology, and (C) VGluT1 expression in the majority of mature neurons after three weeks of differentiation. Scale bar, 100 µm.

Figure 4. Glutamatergic and GABAergic differentiation of human iPSCs. Glutamate and GABA immunocytochemistry in differentiated neurons generated from MSC-iPSC neural progenitors illustrated (A) an increase in the proportion of neurons expressing glutamate in the presence of cyclopamine, whereas (B) a complementary increase in GABAergic differentiation is observed when Shh signaling remained unperturbed. (C) The average proportions of MAP2 positive neuronal cells and glutamate and GABA expressing neurons generated from NPCs in the presence of absence of cyclopamine and FGF-2. The effect of cyclopamine mediated inhibition of Shh was statistically significant for glutamate and GABA expressing neurons, as compared to untreated conditions. * = P < 0.001, ** = P < 0.0001. (D) Expression of TBR1 and (E) VGluT1 in neurons generated from dorsal NPCs. (F) Analysis of differential expression of TBR1 and VGluT1 in the presence or absence of cyclopamine and FGF-2 by RT-PCR. Scale bar: 100 μm.

Figure 5. Electrophysiological assessment of glutamatergic cultures. Electrophysiological recording from cortical neurons generated from (A-C) hESCs and (D, E) MSC-iPSCs. Phase-contrast image of **(**A) hESC-derived, dorsally patterned neuron during patch clamp recordings showing generation of action potentials upon 30 pA current injection after 52 days of differentiation. (B) Voltage steps (−80 mV to 60 mV) elicited inward and outward currents in neurons generated from hESCs. (B) Application of 1 μM of the sodium channel blocker

tetrodotoxin completely eliminated inward currents in neurons generated from hESCs. In addition, (C) administration of 1 mM glutamate evoked inward currents at negative membrane potentials in hESC-derived neuronal populations. (D) Phase contrast image of a dorsally patterned cortical neuron generated from iPSCs firing action potentials upon 30 pA current injection after 52 days of differentiation *in vitro*. (E) In voltage-clamp mode, step depolarizing induced inward and outward currents in iPSC-derived cortical neurons.

Figure 6. Characteristic response of the neuronal populations to Aβ neurotoxicity. (A) Representative phase contrast images of (A) adult rat hippocampal neurons and (B) hESC-derived dorsally patterned cortical neurons treated with 2µM Aβ globulomers, exhibiting neuronal cell death after two and three days, respectively. (C) Glutamatergic neurons exhibited progressively higher cell death with increasing concentrations of the globulomeric form of Aβ, as measured by immunofluorescence staining of activated caspase-3. (D) Quantitative analysis demonstrated a concentration dependent onset of apoptosis in glutamatergic neurons treated with Aβ globulomers. As Aβ concentrations increased, (E) the percentages of glutamatergic neurons and (F) the fraction of neurons with a glutamatergic fate decreased. The line graph insert in panel F shows the progressive decrease of percentages of neurons that belonged to a glutamatergic phenotype with increasing Aβ concentrations. The increases in cell death and the decrease in the total percentages of glutamatergic neurons treated with 1, 2, and 5 µM Aβ globulomers were statistically different compared to untreated cultures. The decrease in the number of MAP2 and glutamate expressing cells was significant in conditions treated with 2, and 5 µM Aβ, as compared to culture that were not treated with Aβ. * = P < 0.005, ** = P < 0.001, *** = P < 0.00-01. Scale bar: 100 µm.

Figure 7. Examination of Aβ binding affinity in aged glutamatergic neurons. Cortical neurons were treated with 5 µM Aβ globulomers for 24 hr, then immunostained with an anti-Aβ antibody. Binding of Aβ globulomers on the surface of MAP2+ neurons at (A) day 25, as compared to (B) day 58 of neuronal maturation illustrates enhanced interaction and binding of Aβ to aged neurons in culture. (C) The untreated control without Aβ showed no signal. Scale bar, 100 µm.

Figure 8. Neuronal phenotype-specific Aβ binding and neurotoxicity. Aβ and MAP2 staining of cultures derived from dorsal and ventral NPCs mainly giving rise to glutamatergic and GABAergic populations, respectively, exposed to globulomers illustrated enhanced binding of Aβ to the (A) glutamatergic populations as compared to (B) GABAergic cultures. The level of Caspase-3 activations was elevated in (C) glutamatergic versus (D) GABAergic cultures. (E) Quantitative analysis of the percentages of MAP2 expressing neurons, number of globulomer aggregates divided by number of cells stained with DAPI, and percentage of cells containing activated caspase-3 in glutamatergic and GABAergic neuronal populations in the presence or absence of Aβ globulomers (5 µM) for 72 hr. Scale bar: 100 µm. (E) In conditions treated with 5 µM Aβ, the overall changes in percentages of MAP2+ and activated caspase-3+ neurons in glutamatergic cultures was significantly different from GABAergic cultures, ** = $P < 0.001$.

Table 1. PCR primer sets used to validate the differential expression of the candidate genes in cortical neural progenitors and maturely differentiated cultures.
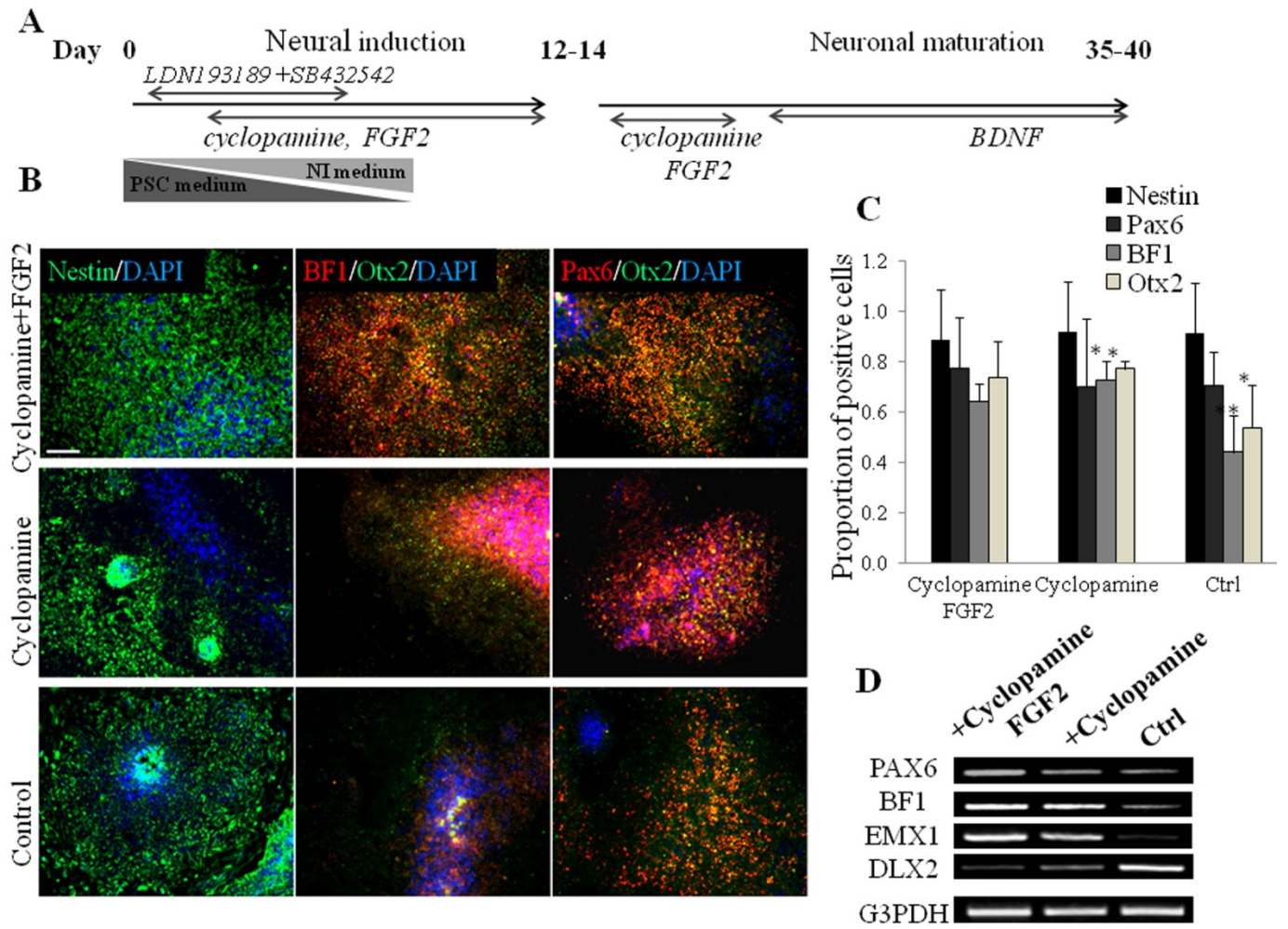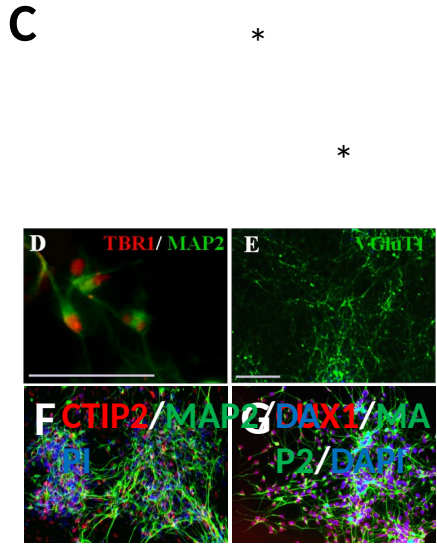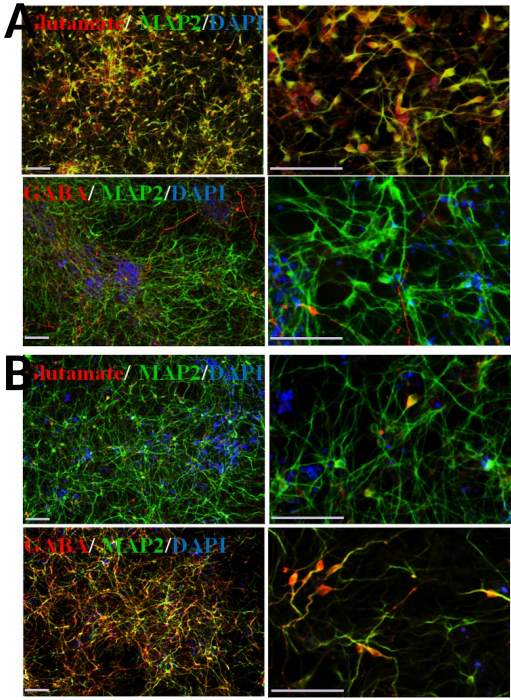
Figure 1

Figure 2

A — Glutamate / MAP2 / DAPI; GABA / MAP2 / DAPI

B — Glutamate / MAP2 / DAPI; GABA / MAP2 / DAPI

C

D — TBR1 / MAP2

E — VGluT1

F — CTIP2 / MAP2 / DAPI

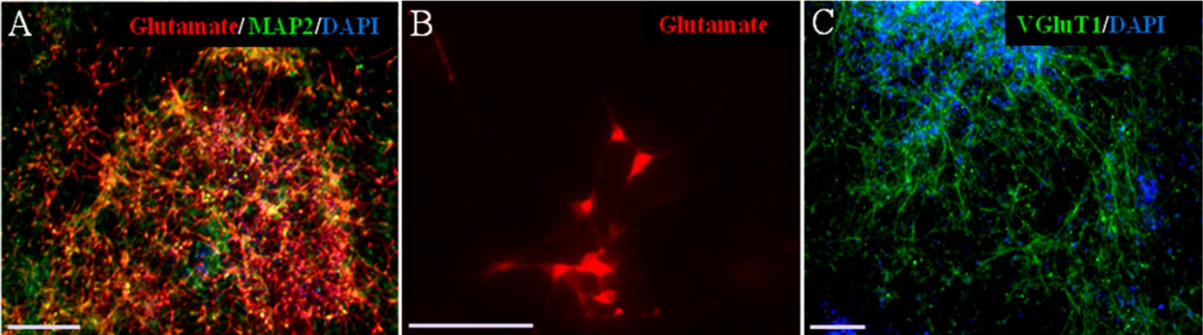G — DAX1 / MAP2 / DAPI

H

TBR1
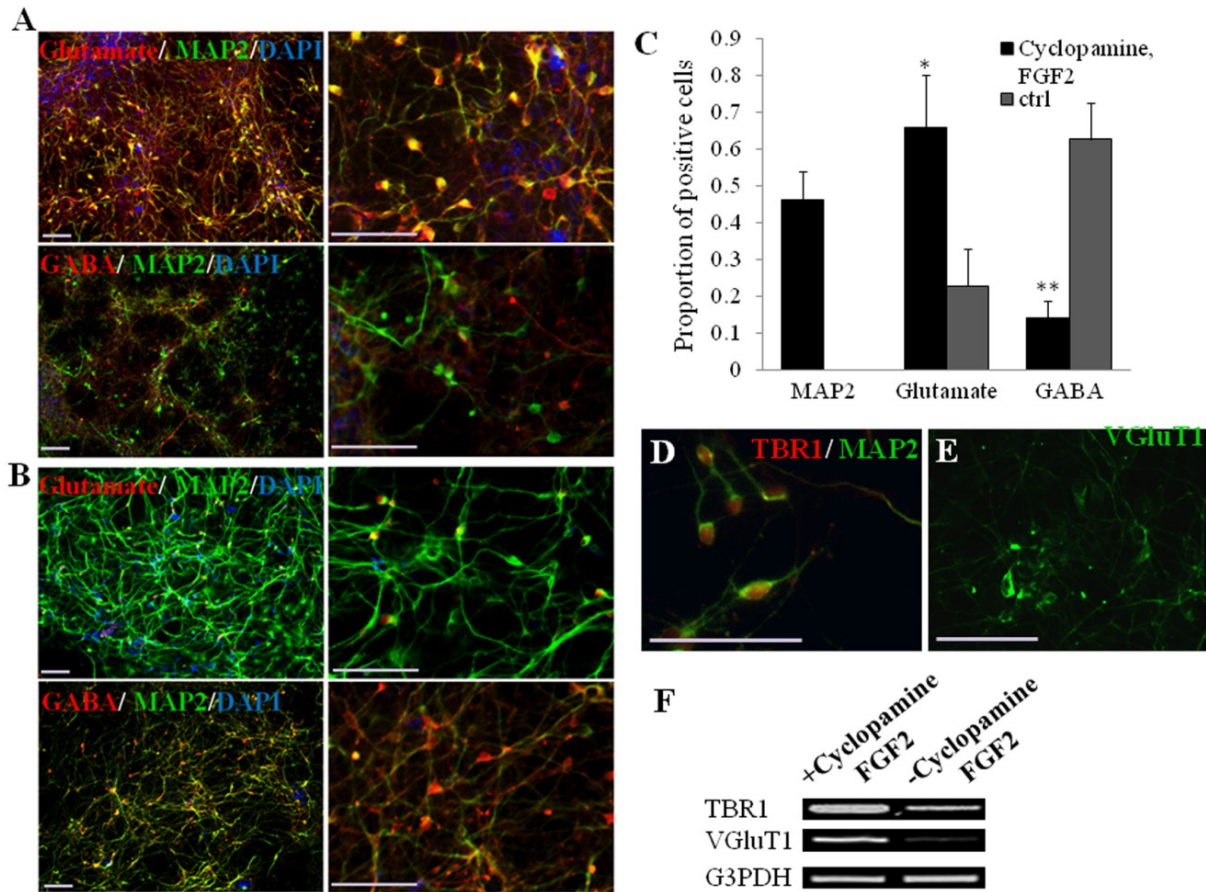
VGluT1

G3PDH

+Cyclopamine +FGF2

Cyclopamine

FGF2

Figure 3.

Figure 4.

Figure 5.
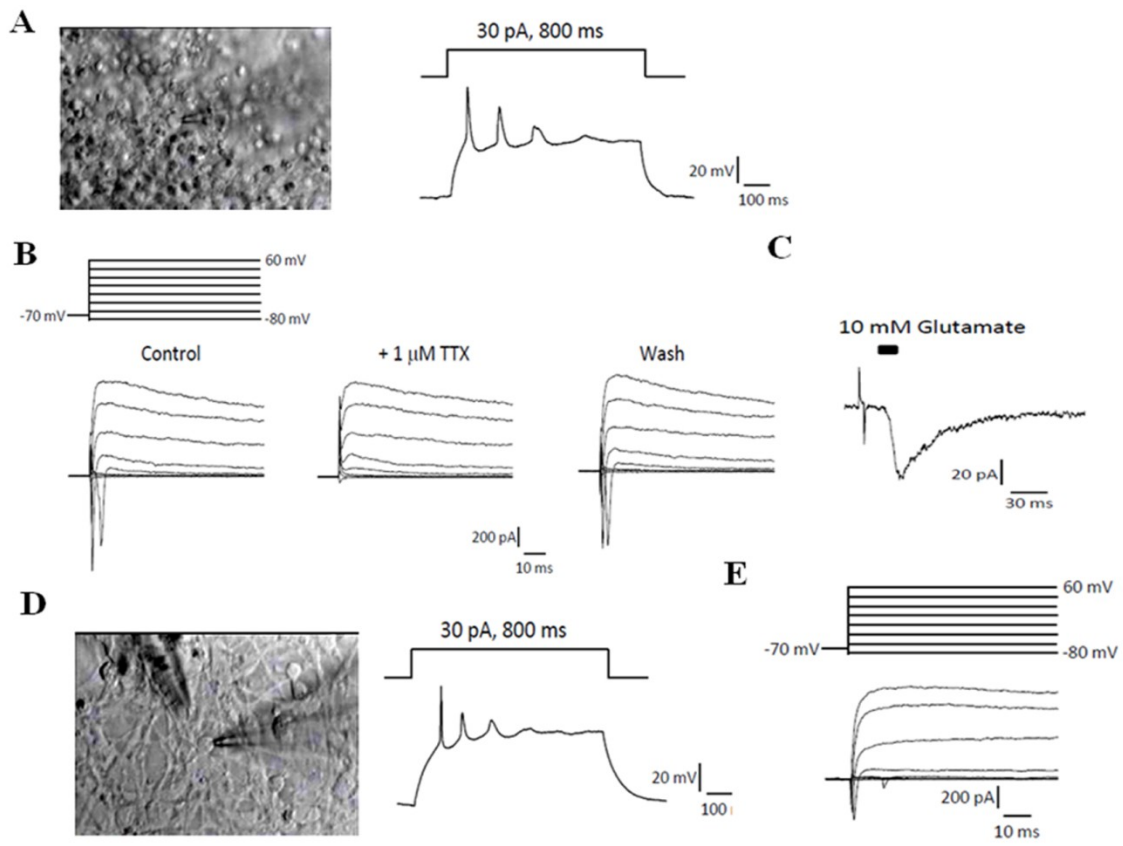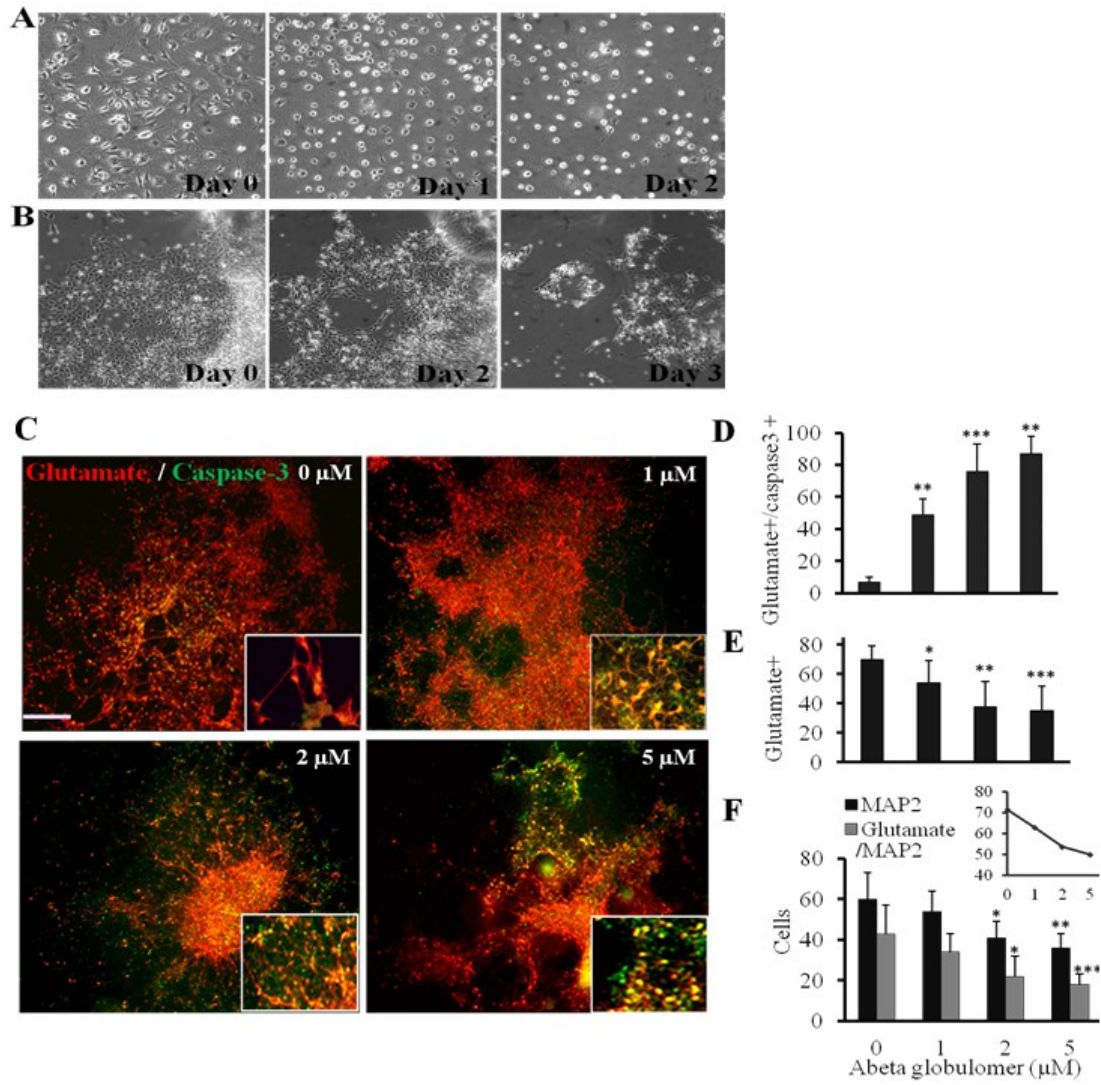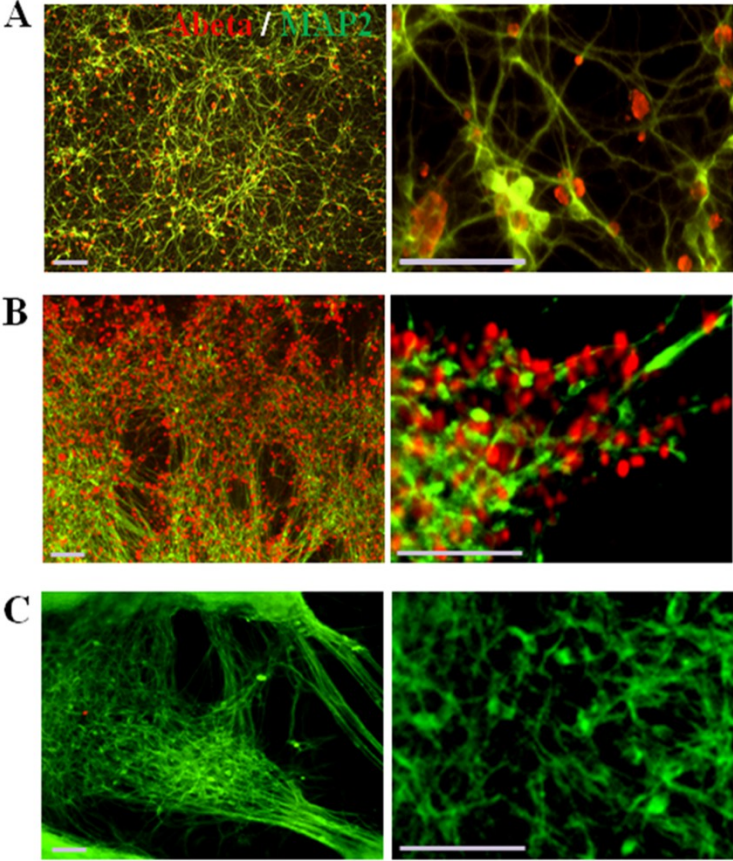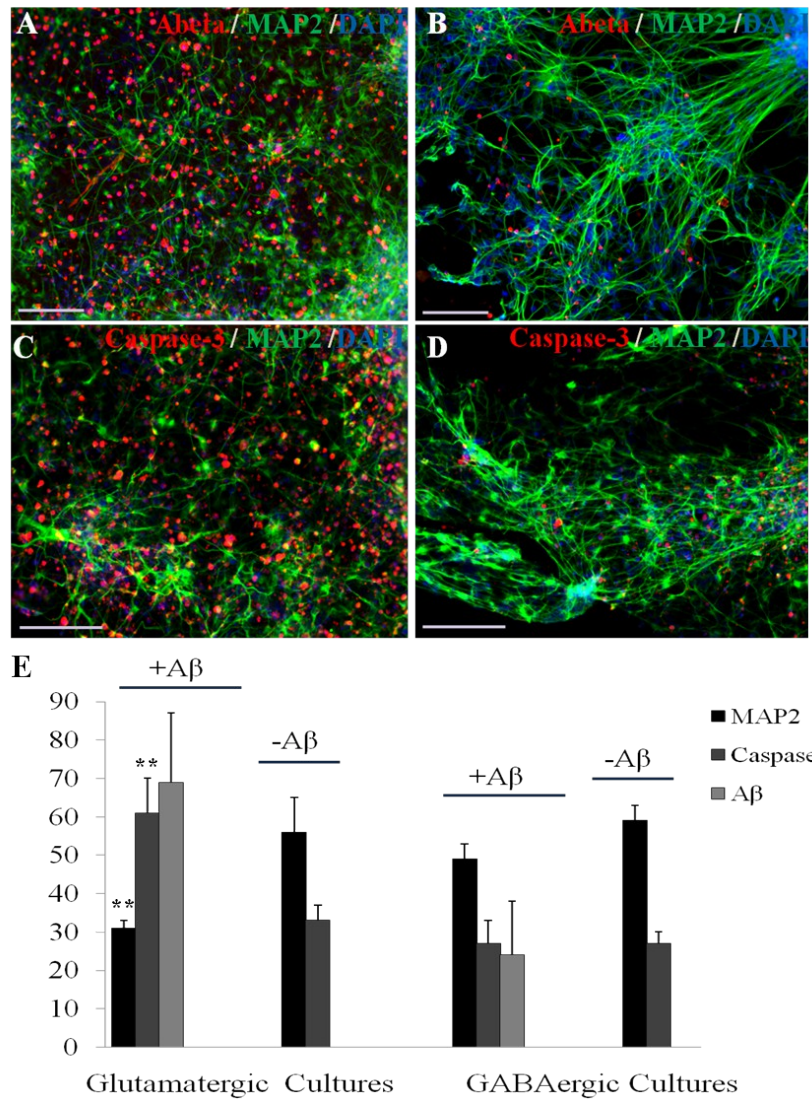
Figure 6.

Figure 7.

Figure 8.

Table 1. Primer sequences.

Primer set Sequenced (5'→ 3')

Gene	Primer Bank ID	Forward	Reverse
PAX6	189083679b3	GTAAACCGAGAGTAGCGACTCC	GCACTCCCGCTTATACTGGG
BF1	32307176b2	GAGCGACGACGTGTTCATC	GCCGTTGTAACTCAAAGTGCTG
EMX1	28279427a1	AAGCGCGGCTTTACCATAGAG	GGGTGAGGGTAGTTGAGCG
DLX2	4758168a3	GCCTGAAATTCGGATAGTGAACG	AGGGGATCTCACCACTTTTCC
TBR1	22547231b1	GCAGCAGCTACCCACATTCA	CGTGCAAGACAAGCTCGGAT
VGluT1	9945322a1	TTTTCTGGGGCTACATTGTCAC	ACTCCGTTCTAAGGGTGGGG
G3PDH	7669492a2	TGTTGCCATCAATGACCCCTT	CTCCACGACGTACTCAGCG